

**Predicting neutron production from cosmic-ray muons**

Y.-F. Wang, V. Balic, and G. Gratta

*Physics Department, Stanford University, Stanford, California 94305*

A. Fassò and S. Roesler

*Stanford Linear Accelerator Center, Stanford, California 94309*

A. Ferrari

*INFN, Sezione di Milano, Via Celoria 16, I-20133, Milano, Italy*

(Received 26 January 2001; published 5 June 2001)

Fast neutrons from cosmic-ray muons are an important background to underground low-energy experiments. The estimate of such a background is often hampered by the difficulty of measuring and calculating neutron production with sufficient accuracy. Indeed substantial disagreement exists between the different analytical calculations performed so far, while data reported by different experiments are not always consistent. We discuss a new unified approach to estimate the neutron yield, the energy spectrum, the multiplicity, and the angular distribution from cosmic muons using the Monte Carlo simulation package FLUKA and show that it gives a good description of most of the existing measurements once the appropriate corrections have been applied.

DOI: 10.1103/PhysRevD.64.013012

PACS number(s): 96.40.Tv, 14.60.Pq, 25.20.-x, 25.40.Sc

**I. INTRODUCTION**

Fast neutrons from cosmic-ray muons represent an important background for low-energy underground experiments such as searches for proton decay and dark matter, and low-energy neutrino oscillation. Unlike charged hadrons which can be tagged by a veto detector system, neutrons usually cannot be identified until they are finally captured, mimicking the signal. The occasional neutron scattering with the sensitive material of the detector and the long lifetime of neutrons in the detector and surrounding materials further complicate the situation. For example, the Palo Verde reactor neutrino oscillation experiment found such neutrons to be their dominant background [1], and a similar situation is expected at the ultralong-base-line detector KamLAND [2]. Low-energy solar neutrino experiments such as SNO and Borexino also have to estimate such backgrounds and the understanding of neutron backgrounds may be relevant in resolving the controversy between the CDMS [3] and DAMA [4] results on dark matter searches. Finally, low-energy accelerator experiments at shallow depths, such as KARMEN, LSND, and OrLaND, have also similar problems.

Although the total neutron yield from cosmic muon spallation has been measured by several experiments, contradictory results are given in the literature [5–9]. Theoretical calculations [9–11] are also not consistent with each other and with the data. The fact that primary neutrons, pions, and protons can all produce secondary neutrons through hadronic interactions makes analytical calculations very difficult. A simple cascade model [11] suggests that the number of nuclear cascade products such as neutrons, pions, and protons increases with the average muon energy approximately like  $E_\mu^{0.7}$ . This formula agrees with most measurements [5–7] except the recent one by the LVD Collaboration [8].

In addition to these problems with neutron yields, the few

measurements of the neutron energy spectrum [8,12] are not well reproduced by theoretical calculations [13,14]. The interpretation of experimental data is complicated by the fact that the neutron energy spectrum depends upon the muon spectrum, which, in turn, is a function of the depth at which the measurement is carried on and the geometrical configuration of the underground site. There is a broad range of results reported in the literature. Barton [13] suggests that the spectrum of neutrons from hadronic cascade follows  $E^{-1/2}$  between 10 and 50 MeV, while the spectrum of neutrons from  $\pi^-$  capture follows a flat spectrum up to 100 MeV. Perkins [14] suggests that the neutron spectrum from muon spallation follows  $E^{-1.6}$ . The combination of  $(9.7E^{-1/2} + 6.0e^{-E/10})$  has been used in a measurement [7] at a shallow site. It has also been suggested [15] to use proton and neutron spectra following  $E^{-1.86}$  as measured at accelerators for photonuclear interactions [16]. Experimentally the KARMEN experiment reported a visible energy spectrum following  $e^{-E/39}$  for spallation neutrons [12] and the LVD experiment reported a visible energy spectrum following  $E^{-1}$ .

In order to put some order in this area, we have studied the neutron yield, the neutron energy spectrum, the multiplicity, and the angular distribution using the 1999 version of the FLUKA [17] Monte Carlo program which is expected to give an accurate description of all the processes involved. It is our intention to provide a unified approach and obtain a reliable estimate of neutron background for experiments at all depths. While we perform the simulation in scintillators in order to compare with experimental data, results should be applicable to other materials with similar atomic numbers.

**II. MUON SPALLATION MODELS**

Fast neutrons from cosmic-ray muons are produced in the following processes.

(a) Muon interactions with nuclei via a virtual photon

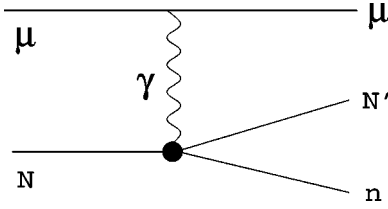


FIG. 1. The Feynman diagram of a muon spallation process.

producing a nuclear disintegration. This process is usually referred to as “muon spallation” and is the main source of theoretical uncertainty.

(b) Muon elastic scattering with neutrons bound in nuclei.

(c) Photonuclear reactions associated with electromagnetic showers generated by muons.

(d) Secondary neutron production following any of the above processes.

Processes (b) and (c) are reasonably well understood while (a) and (d) are the root of the difficulties described in previous calculations. Neutrons can be also produced from muons which stop and are captured, resulting in highly excited isotopes emitting one or more neutrons. This process is reasonably well understood and its contribution to total neutron yield can be calculated. All the experimental results referred to in this paper do not include these neutrons since they can be easily identified and eliminated. Neutron production from neutrinos is negligibly small at the depths considered and thus is not discussed in this paper.

The muon spallation process is schematically illustrated in Fig. 1. The desired  $\mu$ - $N$  cross section is then calculated as

$$\sigma_{\mu-N} = \int \frac{N_{\gamma}(\nu) \sigma_{\gamma-N}^{virt}(\nu)}{\nu} d\nu \quad (1)$$

where  $\nu = E - E'$ ,  $E$  and  $E'$  are energies of initial and final muons, and  $N_{\gamma}(\nu)$  the virtual photon energy spectrum. Theoretical calculations often treat the virtual photons according to the Weizsäcker-Williams approximation [18], in which the passage of a charged particle in a slab of material produces the same effects as a beam of quasireal photons. A general expression of the Weizsäcker-Williams formula is given in Ref. [10]:

$$N_{\gamma}(\nu) = \frac{\alpha}{\pi} \left[ \frac{E^2 + E'^2}{p^2} \ln \frac{EE' + PP' - m^2}{m\nu} - \frac{(E + E')^2}{2P^2} \ln \frac{(P + P')^2}{(E + E')\nu} - \frac{P'}{P} \right], \quad (2)$$

where  $m$  is the muon mass, and  $P$  and  $P'$  are the momenta of initial and final muons.

Since in the above approximation it is assumed that the  $\gamma$ - $N$  cross section is the same for real and virtual photons, the measured  $\gamma$ - $N$  cross section can be used to calculate the  $\mu$ - $N$  cross section in Eq. (1). At low muon energy the situation is more complicated. Here, the virtuality of the photon becomes comparable to its energy and cannot be neglected. It follows that the Weizsäcker-Williams approximation can

no longer be used. In addition, the interaction of the virtual photon with the nucleus is a collective excitation of the nucleus [giant dipole resonance (GDR)] rather than a single photon-nucleon interaction. This implies that the GDR model would have to be applied to virtual photons, introducing further theoretical and technical complications. However, it might be reasonable to assume that neutron production by low-energy muon interactions is small as compared to neutron photoproduction by low-energy bremsstrahlung photons and adds therefore only a minor contribution to the total neutron yield.

In addition to these assumptions, there are a number of problems associated with analytical calculations: first, they cannot reliably calculate all daughter products for every nucleus if the  $\gamma$ - $N$  interaction is very violent so that the nucleus becomes highly excited; second, they cannot properly take into account secondary neutron production. Hence, while these calculations provide useful guidance and, at shallow depths, where hadronic shower effects are small, they may even give quantitatively sound predictions [10], in general they cannot be considered particularly reliable.

Monte Carlo approaches are commonly used to properly model hadronic cascades. Currently the most complete code to describe both hadronic and electromagnetic interactions up to 20 TeV is FLUKA [17]. In this program, different physical models, or event generators, are responsible for the various aspects of particle production at different energies [19]. High-energy hadronic interactions are described based on the dual parton model followed by a preequilibrium-cascade model. In addition, models for nuclear evaporation, breakup of excited fragments, and  $\gamma$  deexcitation treat the disintegration of excited nuclei. Hadronic interactions of photons are simulated in detail from threshold (GDR interactions) up to TeV energies (vector meson dominance model). For nuclei up to copper, measured photonuclear cross sections in the low-energy region are used [21]. Hadronic interactions of muons are based on the Weizsäcker-Williams approximation as formulated by Bezrukov and Bugaev [20]. A spectrum of virtual photons is generated which interact with nuclei similar to real photons. As a result of the above theoretical and technical complications in the description of hadronic interactions of virtual photons at very low energies, the simulation is restricted to photon energies above the delta resonance threshold. The implementation of hadronic interactions of muons has been shown to give reliable predictions for the MACRO experiment [22].

In the following FLUKA is used to obtain a consistent and complete estimate of neutron production from cosmic muons. We model a simple cubic detector filled with liquid scintillator  $C_n H_{2n+2}$ , where  $n$  is taken to be 10. Muons with monochromatic energy are tracked in the detector, and secondary neutrons and other hadrons are analyzed.

### III. NEUTRON YIELD

The total neutron yield is probably the most measured quantity in our problem. There are many experimental results from different depths which can be compared with the model.

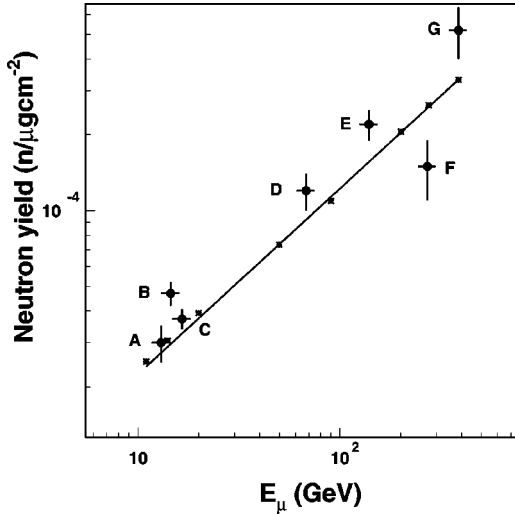


FIG. 2. Neutron production rate as a function of muon energy. The stars indicate the FLUKA simulation with a fit to the power law. The experimental points, with the abscissa corresponding to the average energy at the experiment's depth: (A) 20 meter water equivalent (m.w.e.) [7,6], (B) 25 m.w.e. [23], (C) 32 m.w.e. by the Palo Verde experiment [6], (D) 316 m.w.e. [23], (E) 750 m.w.e. [24], (F) 3650 m.w.e. by the LVD experiment at Gran Sasso [8], and (G) 5200 m.w.e. by the LSD detector at Mont Blanc [5].

All neutrons, either primary or secondary, are included. Double counting due to neutron scattering or neutron spallation is carefully avoided. Because of the limited size of the detection volume in the simulation, some neutrons can escape, resulting in fewer secondary neutrons. The total number of neutrons thus depends on the size of the detector. The detector size has to be limited so that the muon energy loss is small and the initial muon energy can be used as a constant. To correct this problem, we run the simulation with different detector sizes at each muon energy and fit the neutron yield as a function of the percentage of neutrons which escape the detector. An exponential behavior is found and the total number of neutrons can be extrapolated. The corrected neutron yield as a function of the muon energy is shown in Fig. 2. The neutron yield per muon can be fit as

$$N_n = 4.14 E_\mu^{0.74} \times 10^{-6} \text{ neutron}/(\mu\text{g cm}^{-2}), \quad (3)$$

where  $E_\mu$  is in GeV. This relation is consistent with the  $E_\mu^{0.7}$  law suggested in Ref. [11].

While many experiments report their results as a function of the detector's depth underground, clearly the proper physical parameter is the mean muon energy at the detector. The conversion between the two quantities is not entirely trivial as the average energy depends upon the geometry of the overburden, particularly in the case of deep sites. Here for consistency we report all experimental results as a function of the average muon energy  $\bar{E}_\mu$ . For measurements performed at deep laboratories such as Gran Sasso or Mont Blanc the conversion is given in the original papers [5,8], while for shallow sites we estimate the average muon energy loss using the simple relation [25] and assuming a flat geometry:

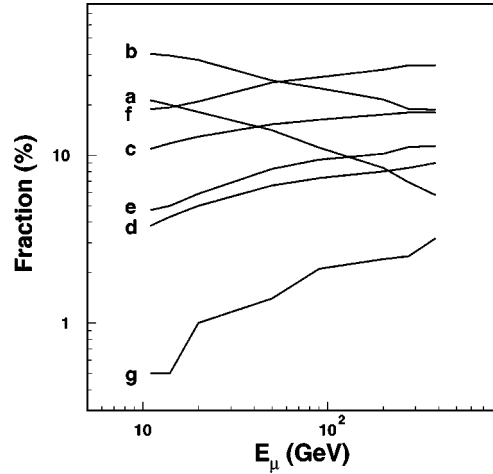


FIG. 3. Origin of neutrons: (a) direct muon spallation, (b) real photonuclear disintegration, (c) neutron spallation, (d) proton spallation, (e)  $\pi^+$  spallation, (f)  $\pi^-$  spallation and capture, and (g) others.

$$\frac{dE_\mu}{dX} = -\alpha - E_\mu/\xi, \quad (4)$$

where  $E_\mu$  is in GeV,  $\alpha = [1.9 + 0.08 \log(E_\mu/m_\mu)] \times 10^{-3} \text{ GeV}/(\text{g cm}^{-2})$  and  $\xi = 2.5 \times 10^5 \text{ g/cm}^2$  in rock. All known experimental neutron-production rates are reported in Fig. 2 along with the FLUKA predictions. The agreement is substantially better than obtained with previous calculations [9,10].

Given this agreement we can proceed to extract from the Monte Carlo simulation information on the origin of the neutrons. This is of great interest as it can provide hints for a better theoretical understanding of the processes involved. In Fig. 3 we show the fractional composition of the neutrons by origin. As expected the fraction of neutrons from primary processes such as muon spallation and real photonuclear interactions decreases with energy, while secondary neutrons from neutron and proton spallation, from pion absorption, and from other minor processes such as  $\Lambda$  and  $\Sigma$  decays increase in relative importance with energy.

The  $\pi^+$  yield in muon spallation can be estimated from analytical calculations more reliably than that of neutrons. This is because (1) secondary processes for neutrons are more important; (2) there is an uncertainty in the direct neutron production from virtual or real pions. Table I shows the comparison of our simulation with an analytical calculation [10] which does not include secondary pions from hadronic showers. In the experimental data [7],  $\pi^+$ 's are identified through their  $\pi^+ \rightarrow \mu^+ \rightarrow e^+$  decays, and hadronic shower effects are not corrected for. In the pion case, good agreement between data, FLUKA, and the analytical calculation can be seen at shallow depth, where secondary hadrons from showers are not important. We obtained the pion yield per muon as

$$N_{\pi^+} = 4.45 \times E_\mu^{0.80} \times 10^{-7} \text{ pion}/(\mu\text{g cm}^{-2}), \quad (5)$$

TABLE I. Neutron and  $\pi^+$  yields [in units of  $10^{-5}/(\text{g cm}^{-2})$ ] per muon at different depths. Note that the analytical calculation [10] does not include real photon-nuclear disintegration and secondary particles.

Depth (m)	20		100		500	
	$n$	$\pi^+$	$n$	$\pi^+$	$n$	$\pi^+$
Energy (GeV)	10.3		22.4		80.0	
Yield						
Anal. calc. [10]	0.87	0.30	1.21	0.45	2.08	0.86
FLUKA	2.5	0.31	3.9	0.52	11.0	1.51
Data [7]	$3.0 \pm 0.5$		$0.35 \pm 0.07$			

where  $E_\mu$  is in GeV. Again, this is consistent with the  $E_\mu^{0.7}$  universal law suggested by Ryazhskaya and Zatsepin [11] and the results from Ref. [24].

#### IV. NEUTRON ENERGY SPECTRUM

The neutron energy spectrum is particularly controversial, with a wide range of results reported in theoretical calculations and in the few experimental measurements. In Fig. 4 we show some of the energy spectra obtained with FLUKA. Each histogram is fitted to the universal empirical function

$$\frac{dN}{dE_n} = A \left( \frac{e^{-7E_n}}{E_n} + B(E_\mu) e^{-2E_n} \right), \quad (6)$$

where  $A$  is a normalization factor and

$$B(E_\mu) = 0.52 - 0.58 e^{-0.0099E_\mu}. \quad (7)$$

This simple function reproduces fairly well the FLUKA distributions with  $\chi^2$  per degree of freedom of 3.9, 4.5, 9.6, and 3.7 for 11, 20, 90, and 270 GeV, respectively.

We are aware of two direct measurements that can be compared to our calculations, as shown in Fig. 5. The KAR-

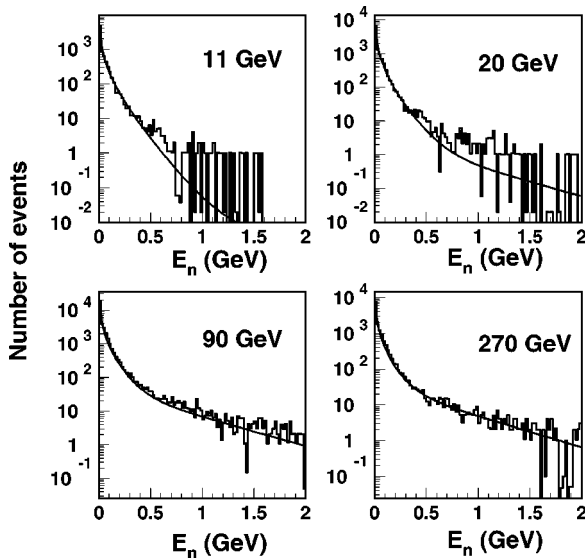


FIG. 4. Energy spectrum of neutrons at different muon energies together with our parameterization. We find  $\chi^2/N_{\text{DF}}$  of 3.9, 4.5, 9.6, and 3.7 for 11, 20, 90, and 270 GeV, respectively.

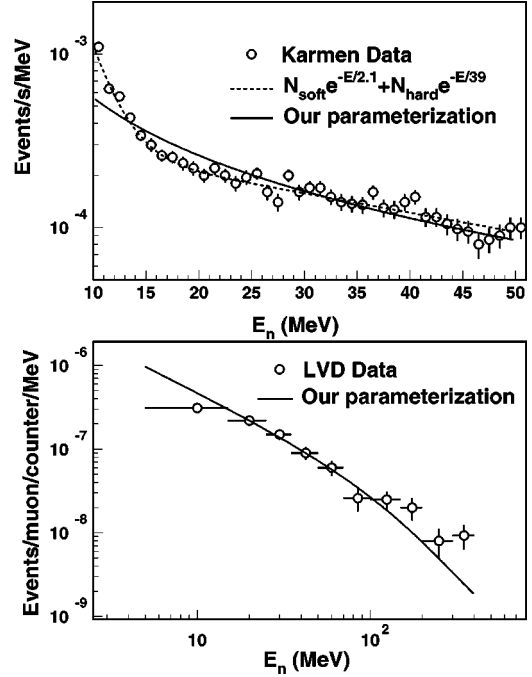


FIG. 5. Comparison of measured neutron energy spectrum with our parameterization.

MEN Collaboration measured the neutron energy spectrum up to 50 MeV [12]. Within this modest range, their parameterization  $N_{\text{soft}} e^{-E_n/2.1} + N_{\text{hard}} e^{-E_n/39}$  is in a reasonable agreement with our result. They attribute all the soft component to muon capture but it seems that muon spallation also produces some soft neutrons. The LVD experiment reported a  $E_n^{-1}$  spectrum [8] up to 400 MeV, also in a reasonable agreement with our result.

Some of the theoretical estimates of neutron energy spectrum are comparable to our results at low energies while our calculation gives results over a much wider range of energies. For example, the power laws  $E_n^{-1.6}$  [14] and  $E_n^{-1.86}$  [15] agree with our results up to 400 MeV. Other functions, such as  $(9.7E_n^{-1/2} + 6.0e^{-E_n/10})$  [7] or that suggested by Barton [13], are significantly different.

#### V. NEUTRON MULTIPLICITY AND ANGULAR DISTRIBUTION

The neutron multiplicity is probably the least known quantity in the neutron production problem. In most cases muon spallation only happens once and produces only a few primary hadrons. But these hadrons can shower and generate secondary hadrons, including neutrons. Using our simulation we have found that in some cases the number of secondary neutrons exceeds 50. The average number of neutrons is about 3 for a 11 GeV muon, and it increases to about 7 at a muon energy of 385 GeV. Figure 6 shows the neutron multiplicity distributions at different muon energies from FLUKA, together with the universal empirical parameterization

$$\frac{dN}{dM} = A [e^{-A(E_\mu)M} + B(E_\mu) e^{-C(E_\mu)M}], \quad (8)$$

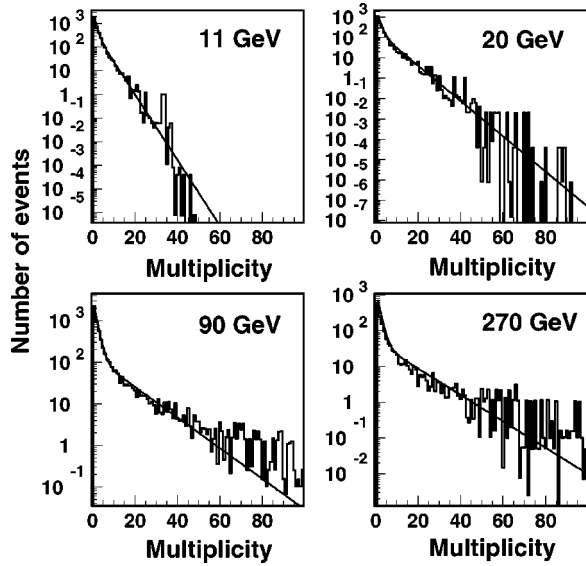


FIG. 6. Neutron multiplicity at different muon energies together with our parametrization. We find  $\chi^2/N_{\text{DF}}$  of 0.6, 2.0, 1.5, and 1.5 for 11, 20, 90, and 270 GeV, respectively.

where  $M$  is the multiplicity:

$$A(E_\mu) = 0.085 + 0.54e^{-0.075E_\mu}, \quad (9)$$

$$B(E_\mu) = \frac{27.2}{1 + 7.2e^{-0.076E_\mu}}, \quad (10)$$

$$C(E_\mu) = 0.67 + 1.4e^{-0.12E_\mu}. \quad (11)$$

The  $\chi^2$ 's per degree of freedom are 0.6, 2.0, 1.5, and 1.5 for 11, 20, 90, and 270 GeV, respectively.

There are only few experimental results [6] on multiplicity. The Palo Verde experiment at the shallow depth corresponding to a mean muon energy of about 16.5 GeV observed a two-neutron to one-neutron ratio between 5 and 10, depending on the assumption on three-neutron yield. Similar results are also reported by Bezrukov *et al.* [23]. These numbers appear to be substantially larger than the FLUKA prediction of 2. While more data would be desirable to better understand this discrepancy it is possible that the data are affected by the incomplete efficiency matrix for four or more neutrons, whose contribution, previously assumed small, seems significant from our simulation.

There are no experimental results on the neutron angular distribution with respect to muons. Experimental results [26] on  $\gamma + {}^{12}\text{C} \rightarrow p + X$  have been used [15] as a first approximation of the neutron angular distribution. The distribution is expected to be forward peaked, smoothed somewhat by the contribution of secondary neutrons. Our simulation is well parametrized by the angular distribution

$$\frac{dN}{d \cos \theta} = \frac{A}{(1 - \cos \theta)^{0.6} + B(E_\mu)}, \quad (12)$$

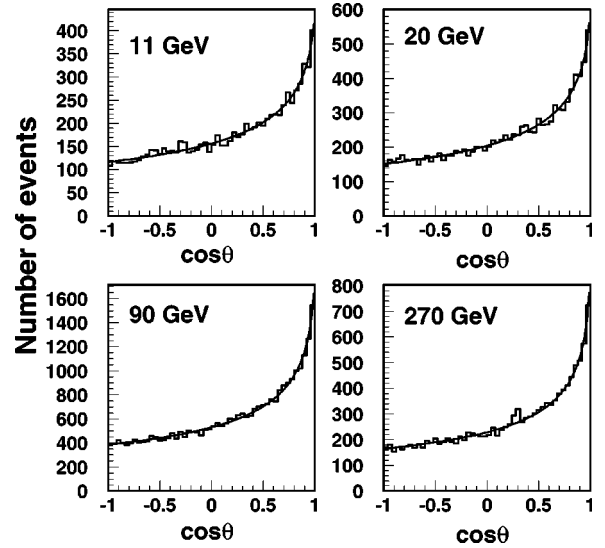


FIG. 7. Neutron angular distributions with respect to the muon direction at different muon energies together with our parametrization. We find  $\chi^2/N_{\text{DF}}$  of 0.51, 0.51, 0.72 and 0.72 for 11, 20, 90 and 270 GeV respectively.

where  $B(E_\mu) = 0.699E_\mu^{-0.136}$ . Figure 7 shows the  $\cos \theta$  distribution at the usual set of energies together with the above parametrization. The  $\chi^2$  per degree of freedom are 0.51, 0.51, 0.72, and 0.72 for 11, 20, 90, and 270 GeV, respectively.

## VI. SUMMARY

We obtained for the first time a complete description of neutron production from cosmic-ray muons using the FLUKA Monte Carlo program. Results have been compared with existing data and some analytical calculations reported in the literature. With a few exceptions, our results agree well with the data, and our predictions cover an energy range much broader than what has been discussed before.

Analytical parametrizations have been obtained for neutron yield, energy spectrum, multiplicity, and angular distribution. These formulas can be used as a starting point to estimate neutron backgrounds from cosmic-ray muons when the muon energy spectrum is known. For detailed calculations of the muon-induced neutron backgrounds in low-energy underground experiments, a complete Monte Carlo simulation is needed to account for the correlation among different variables and can be set up using FLUKA. Intermediate processes such as neutron scattering before neutron spallation are also automatically taken into account in this method, which has great promise to improve the quality of predictions.

## ACKNOWLEDGMENTS

We would like to thank P. Vogel for many useful discussions. This work was supported in part by DOE grants DE-FG03-96ER40986 and DE-AC03-76SF00515.

- [1] F. Boehm *et al.*, Phys. Rev. Lett. **84**, 3764 (2000); F. Boehm *et al.*, Phys. Rev. D **62**, 072002 (2000).
- [2] P. Alivisatos *et al.*, “KamLAND: a Liquid Scintillator Anti-Neutrino Detector at the Kamioka site,” Report No. Stanford-HEP-98-03, Tohoku-RCNS-98-15.
- [3] R. Abusaidi *et al.*, Nucl. Instrum. Methods Phys. Res. A **444**, 345 (2000).
- [4] R. Bernabei *et al.*, Phys. Lett. B **480**, 23 (2000).
- [5] M. Aglietta *et al.*, Nuovo Cimento Soc. Ital. Fis., C **12**, 467 (1989).
- [6] F. Boehm *et al.*, Phys. Rev. D **62**, 092005 (2000).
- [7] R. Hertenberger, M. Chen, and B.L. Dougherty, Phys. Rev. C **52**, 3449 (1995).
- [8] M. Aglietta *et al.*, in Proceedings of the 26th International Cosmic Ray Conference, Salt Lake City, 1999, edited by D. Kieda, M. Salamon, and B. Dingus, Vol. 2, p. 44, hep-ex/9905047.
- [9] O.C. Allkofer and R.D. Andresen, Nucl. Phys. **B8**, 402 (1968).
- [10] J. Delorme *et al.*, Phys. Rev. C **52**, 2222 (1995).
- [11] O.G. Ryazhskaya and G.T. Zatsepin, Izv. Akad. Nauk SSSR, Ser. Fiz. **29**, 1946 (1965); in Proceedings of the IX International Conference on Cosmic Rays, London, 1965, Vol. 21, p. 987.
- [12] J. Rapp, Ph.D. thesis, University of Karlsruhe, 1996.
- [13] J.C. Barton, in *Proceedings of the 19th International Conference on Cosmic Rays*, La Jolla, 1985, edited by F. C. Jones (Physical Society, London, 1985), p. 98.
- [14] D.H. Perkins, “Calculation of neutron background in Soudan 2,” 1990.
- [15] Y.F. Wang *et al.*, Phys. Rev. D **62**, 013012 (2000).
- [16] F.F. Khalchukov *et al.*, Nuovo Cimento Soc. Ital. Fis., C **6**, 320 (1983).
- [17] A. Fassò *et al.*, *Proceedings of the 3rd Workshop on Simulating Accelerator Radiation Environments (SARE 3)*, edited by H. Hirayama, KEK Proceedings No. 97-5 (KEK, Tsukuba, Japan, 1997), p. 32.
- [18] C.F. Weizsäcker, Z. Phys. **88**, 612 (1934); E.J. Williams, K. Dan. Vidensk. Selsk. Mat. Fys. Medd. **13**, 4 (1935).
- [19] A. Ferrari and P.R. Sala, in *Proceedings of the Workshop on Nuclear Reaction Data and Nuclear Reaction Physics*, edited by A. Gandini and G. Reffo (World Scientific, Singapore, 1998), Vol. 2, p. 424.
- [20] L.B. Bezrukov and É.V. Bugaev, Yad. Fiz. **33**, 1195 (1981) [Sov. J. Nucl. Phys. **33**, 635 (1981)].
- [21] A. Fassò *et al.*, in Proceedings of the 3rd Specialists Meeting on Shielding Aspects of Accelerator Target and Irradiation Facilities (SATIF3), Tohoku University, Sendai, Report No. OECD-NEA, 1998, p. 61.
- [22] G. Battistoni *et al.*, in Proceedings of Vulcano Workshop on Frontier Objects in Astrophysics and Particle Physics, 1998, hep-ex/9809006.
- [23] L.B. Bezrukov *et al.*, Yad. Fiz. **17**, 98 (1973) [Sov. J. Nucl. Phys. **17**, 51 (1973)].
- [24] R.I. Enikeev *et al.*, Yad. Fiz. **46**, 1492 (1987) [Sov. J. Nucl. Phys. **46**, 883 (1987)].
- [25] T.K. Gaisser, *Cosmic Rays and Particle Physics* (Cambridge University Press, Cambridge, England, 1990), p. 76.
- [26] K.V. Alanakyan *et al.*, Yad. Fiz. **34**, 1494 (1981) [Sov. J. Nucl. Phys. **34**, 828 (1981)].